Mineralogy of Multiple Volcanic episodes of Mare Orientale. S. M. Patel[1], Harish[1], D. D. Patel[2], P. M. Solanki[2], and M. R. El-maarry[1]. [1]Space and Planetary Science Center and Department of Earth Sciences, Khalifa University, Abu Dhabi, UAE (shreekumari.patel@ku.ac.ae), [2]M. G. Science Institute, Ahmedabad, India.

Introduction: Lunar volcanic history is a key to understanding lunar thermal and geological evolution [1]. A total of 17% of the lunar surface is covered by 23 lunar maria [2], lying within or adjacent to large impact basins. Most of the lunar maria (20 out of 23) are located in the PKT, and the remaining three (i.e., Mare Orientale, Mare Moscoviense, and Mare Ingenii) are located in the highlands [3]. The generation, ascent and eruption of mare basalt magma have been the subject of intense study and debate for many years. Spectroscopists have studied and shown the mineralogical diversity of mare basalts [e.g., 4,5,6,7,8].

The Mare Orientale multiring impact basin is located on the western limb of the transitional region between the Moon's thin nearside and thick far-side crust (Figure 1). The circular Orientale Basin was formed in the Imbrium period and has four ring structures [5]. Orientale offers excellent insights into the initial stages of mare emplacement due to its incomplete flooding [8]. Previous researchers have carried out detailed studies on the mineralogy and topography of the Orientale Basin; however, the pyroxene chemistry of the basaltic units in the Mare Orientale has not been explored further. The present study aims to determine the chemical variations among the basaltic units in the Volcanic deposits of Orientale Basin based on the pyroxene chemistry and FeO and TiO_2. The relationship between the pyroxene chemistry and the ages of the basaltic units have been also studied, which further offers us evidence about the chemical evolution of units of distinct ages within the Mare Orientale.

Data and Methods: We used data from the Moon Mineralogical Mapper (M^3) onboard the Chandrayaan-1 mission. M^3 images used in this study were from 100 km altitude at a resolution of ~140m/pixel with 85 spectral bands covering the 0.43-3.0 µm wavelength region [9]. IBD map was generated using [10] to delineate units. Band parameters such as Band Center (BC), Band Area (BA) and Band Depth (BD) were calculated by fitting a fourth-order polynomial line to each spectrum [11, 12, 13 14]. [11] and [12] developed calibrations equations to eliminate the olivine effect from Band I center value of the olivine and pyroxene mixed phase in the spectra. The estimated Band I center (olivine corrected) and Band II center values are applied to calculate the molar Ca, Fe, and Mg content in pyroxenes using a set of equations given by [12] to project those values in pyroxene quadrilateral. [15] created a graphical two-pyroxene thermometer to study the chemical fluctuation of pyroxene, crystallization history, and cooling temperature. FeO content was extracted using the M^3 data following the spectral characteristic angle parameters [16]. For TiO_2 content retrieval, [16] used shukuratov's model.

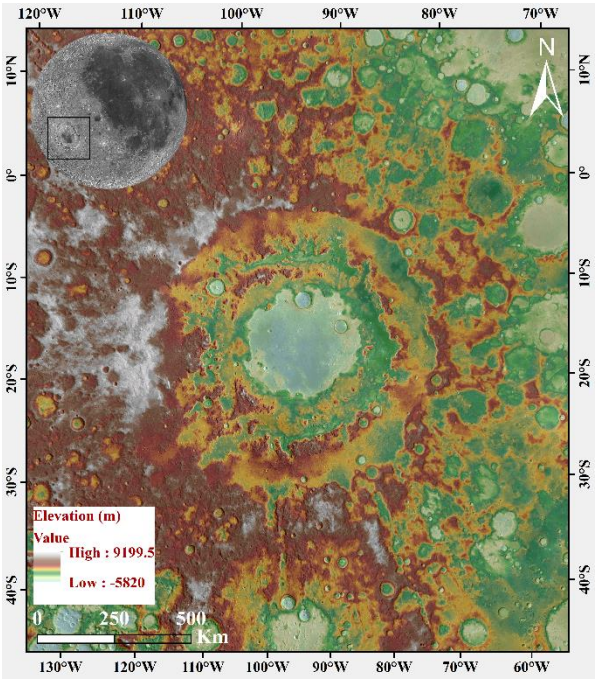

Figure 1: The inset Lunar Reconnaissance Orbiter Camera (LROC) Wide Angle Camera (WAC) map displays the Mare Orientale of the Moon. The Orientale basin (Black box) is located on the far-side of the Moon. Colour-coded LRO-LOLA and Kaguya Terrain Camera Merge DEM of the Orientale show the basin's topography. (Projection: Inset- Orthographic projection centered at 0ºN, 300ºE, stereographic projection centered at 19.4 ºS, 92.8 ºW).

Results and Discussion: Albedo and IBD maps were used to delineate the different mare units of the Orientale basin (Figure 2). We collected ~181 mafic spectra from the basaltic units of the basin to characterize the composition of volcanic rock-basalt. Most samples illustrate evidence of olivine and pyroxene mixture spectra. Hence a correction factor was applied to the Band I center to eliminate the possible contribution of the olivine. The values from band parameters reveal the compositional trend of clinopyroxenes. The estimated band center of the

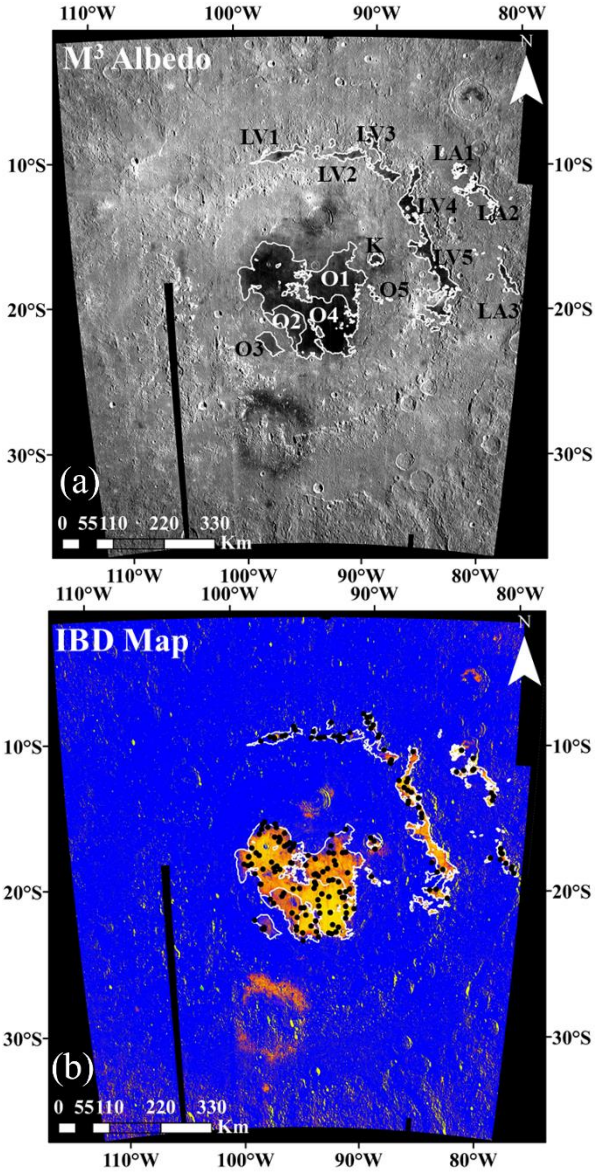

Figure 2: (a) M3 1578 albedo map showing the albedo variations among the basaltic units. (b) M3 colour composite image (red: IBD 1000, green: IBD 2000, and blue: R1578) display the mineralogical variations amongst the mare units. The solid white lines demarcate the boundaries of the distinct mare units.

pyroxene is used to calculate the relative abundance of the pyroxene compositions. The values are projected onto a pyroxene quadrilateral plot to comprehend the relative proportions of Ca, Mg and Fe content. In the pyroxene quadrilateral plot (Figure 3), the average composition in the Mare Orientale and Kopff crater is $En_{33.15}Fs_{38.75}Wo_{28.09}$ and $En_{33.03}Fs_{30.43}Wo_{34.54}$, respectively; which indicates crystallization of sub-calcic ferroaugite and augite. The crystallization temperature of the basaltic units is between ~1200ºC and 800ºC. In Mare Orientale, FeO content ranges from ~9.8 to 17.6 wt% and TiO_2 content between ~2 and 7 wt%, suggesting the presence of low to medium TiO_2 basaltic deposits.

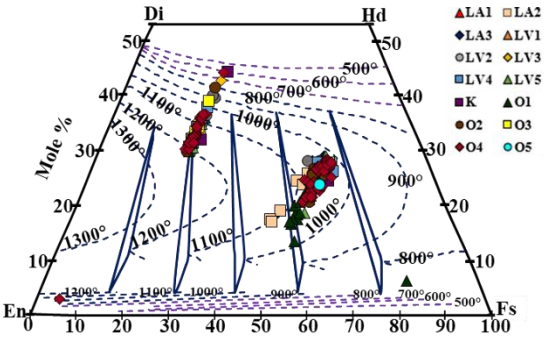

Figure 3: Pyroxene quadrilateral plot showing the mole % composition of endmember temperature pyroxenes from the individual mare units.

Concluding Remarks: The pyroxene band parameter analysis indicated the dominance of clinopyroxenes in the region. The major components in these basaltic units are sub-calcic ferroaugite and augite. The chemical trend of pyroxene compositions suggests that multiple volcanic events have occurred in the Mare Orientale. Few units crystallized from Mg and Ca-rich source magma, whereas few units formed from Fe-enriched source. Hence, it can be concluded that magmas of different chemical nature are derived from a heterogeneous source.

Acknowledgements: S. M. Patel, Harish, and M. R. El-maarry acknowledge support for this work through an internal grant (8474000336-KU-SPSC). D. D. Patel and P. M. Solanki are thankful to the M. G. Science for all the support.

References: [1] Moriarty, D. P. et al. (2021), *Nat. Commun., 12*, 4659. [2] Head, J. W. and Hawke, B. R. (1975), *VI Lunar Science Conference, 6, 2483-2501*. [3] Arviazhagan, S. (2015), *Planetary Exploration and Science: Recent Results and Advances, 21-43*. [4] Karti, A. and Arivazhagan, S. (2022), *Icarus, 375, 114844.* [5] Liu, J. (2022), *Remote Sensing, 14, 1426.* [6] Lucey, P. (2006), *Reviews in Mineralogy and Geochemistry, 60, 83-219.* [7] Pieters, C. M. (1978), *LPSC, 2825-2849.* [8] Whitten, J. et al. (2011), *J. Geophys. Res., 116, E00G09.* [9] Pieters, C. M. et al. (2009) *Curr. Sci., 96, 4, 500-505.* [10] Mustard, J. F. et al. (2011), *J. Geophys. Res.:Planets, 116(E6).* [11] Cloutis, E. A. (1986), *J. Geophys. Res., 91, 11641*. [12] Gaffey, M. J. (2002), *Asteroids III, 183-204.* [13] Kaur, P. et al. (2013), *Icarus, 222, 137-148.* [14] Thesniya, P. M. (2020), *Meterorit Planet Sci, 55, 2375-2403.* [15] Lindsley, D. H. and Anderson, D. J. (1983), *J. Geophys. Res., 88, A887.* [16] Zhang, W. and Bowels, N. E. (2013), *EPSC, #Abstract 374.*